A Head-to-Head Comparison of Eneamide and Epoxyamide Inhibitors of Glucosamine-6-Phosphate Synthase from the Dapdiamide Biosynthetic Pathway.

Marie A. Hollenhorst, Ioanna Ntai, Bernard Badet, Neil L. Kelleher, and Christopher T. Walsh.

SUPPORTING INFORMATION

Table of Contents *Page*

I. Background Schemes

Scheme S1. Acyl-DAP dipeptide natural products. A) The dapdiamide family of antibiotics, isolated from heterologous expression of a gene cluster from the genome of *P. agglomerans* CU0119 in *E. coli* (*1*). B) Other acyl-DAP dipeptide natural products. N_β-epoxysuccinamoyl-DAP-Val (referred to in the literature variously as CB-25-I, 2-amino-3-(oxirane-2,3-dicarboxamido)-propanoyl-valine, and herbicolin I) has been isolated from *Serratia plymuthica* (*2*) as well as several strains of *P. agglomerans* (*3*) (48b/90, C9-1, and 39b/90). A19009 has been isolated from *Streptomyces collinus* (*4, 5*). Sch37137 is from *Micromonospora* sp., SCC1792 (*6, 7*).

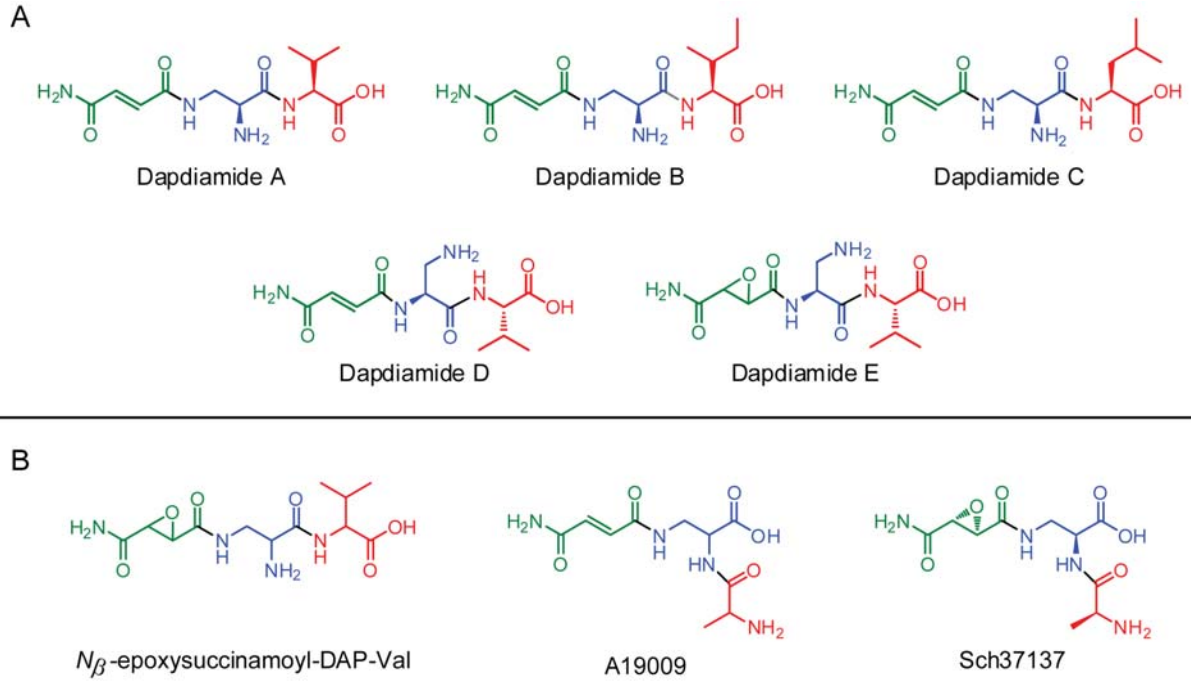

Scheme S2. Biosynthetic route to **1** and **2** (*8, 9*).

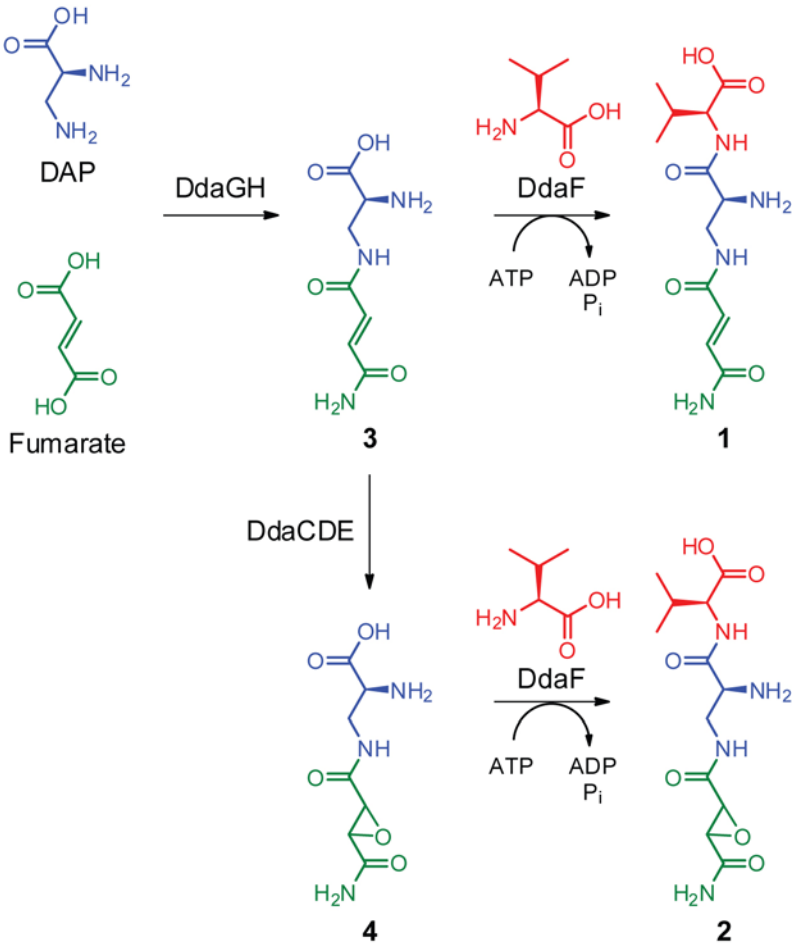

Scheme S3. N_{β}-methoxyfumaroyl-DAP-aa.

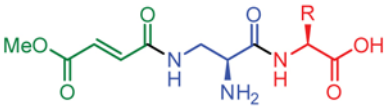

Scheme S4. GlcN6P synthase mechanism.

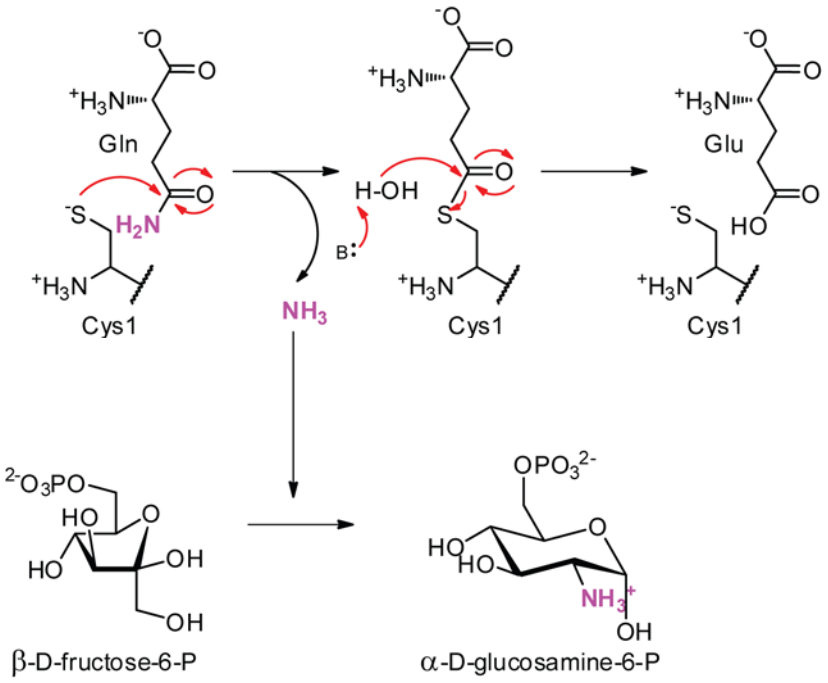

II. Materials and General Methods

E. coli GlmS was purified as described previously (*10*). ***RR*-4**, ***SS*-4**, **3**, and N_α-fumaramoyl-DAP were synthesized as described previously (*8, 9*). **1** (dapdiamide A) was provided by Jessica Dawlaty (Harvard Medical School, Boston, MA) (*1*). Stock solutions of **3** and N_α-fumaramoyl-DAP were prepared by adding 50 mM borate (pH 9.5) to the solid compounds, then heating at approximately 50 °C for several minutes to dissolve. Stock solutions of **1** and ***RR*-2** were prepared by adding dimethyl sulfoxide (DMSO). L-glutamic dehydrogenase (GDH) Type II from bovine liver was purchased as a buffered aqueous solution from Sigma.

III. GlmS Time-Dependent Inactivation Assays

Method. *Assay for time-dependent inhibition of GlmS glutaminase activity.*

Incubation mixtures (30 µL) contained 1.25 µM GlmS, 1 mM ethylenediaminetetraacetic acid (EDTA), 10 mM fructose-6-phosphate (Fru6P), 1 mM tris(2-carboxyethyl)phosphine (TCEP), 100 mM potassium phosphate (pH 7.2), and various inhibitor concentrations. Reactions containing **3**, ***RR*-4**, ***SS*-4**, and N_α-fumaramoyl-DAP additionally contained 5 mM sodium borate (pH 9.5) and were compared to control reactions containing 5 mM sodium borate (pH 9.5). Reactions containing **1** and ***RR*-2** additionally contained 1.2% DMSO and were compared to control reactions containing 1.2% DMSO. The incubations were initiated by addition of GlmS and incubated at room temperature.

After 1, 6, 11, 16, and 21 min, 2 µL of the incubation mixture was added to 98 µL of assay mixture in a 96 well plate that had been preincubated at 37 °C. Assay mixtures contained 1 mM 3-acetylpyridine adenine dinucleotide (APAD), 48 units/mL GDH, 10 mM Fru6P, 10 mM L-Gln, 50 mM KCl, 1 mM EDTA, and 50 mM potassium phosphate (pH 7.5). Reduction of APAD to APADH was monitored continuously for 3 min at 37 °C in a Molecular Devices SpectraMax PLUS or SpectraMax 340PC384 96-well plate reader by measuring the absorbance at 365 nm every 15 s. Relative initial velocities were determined as the slope of the linear portion of each absorbance *vs.* time plot (Figure S1A,B). Each slope was then divided by the relative initial velocity from the no inhibitor incubation aliquot at 1 min to determine a percent activity. Next, a plot of ln(% Activity) *vs.* time of aliquot was generated for each inhibitor concentration (Figure S1C). The slopes of the lines from this plot were multiplied by -1 to yield k_{obs} values. A plot of k_{obs} *vs.* [inhibitor] was generated, and the slope of this line was taken as k_{inact}/K_{irr} (Figure S1D). Reported k_{inact}/K_{irr} values are the average ± standard deviation of two experiments for **3** and ***SS*-4** and three experiments for ***RR*-4**.

A control was performed in which GlmS was not preincubated with inhibitor, but instead immediately assayed with the same final concentration of substrates and inhibitor as in the assay samples. The slopes of the absorbance *vs.* time plots were not found to significantly differ in the presence or absence of inhibitors, demonstrating that continued inhibition did not occur during the enzymatic assay.

The k_{inact}/K_{irr} determined for **3** was 2-fold lower than the value previously reported by Badet and co-workers (*11*). We tested **3** that was used in that study side by side against the newly synthesized compound and found a comparable k_{inact}/K_{irr} of 34 $M^{-1}s^{-1}$, so we used the more recently determined value as a basis for comparison.

Figure S1. Representative plots used to derive inhibitor k_{inact}/K_{irr} values. A) Raw progress curve for a sample taken from incubation of GlmS with no inhibitor at t = 1 min. B) Linear portion of progress curve in panel A used to generate slope. C) Plot of ln(% Activity) *vs.* time for various concentrations of **3**. D) k_{obs} *vs.* [**3**] plot.

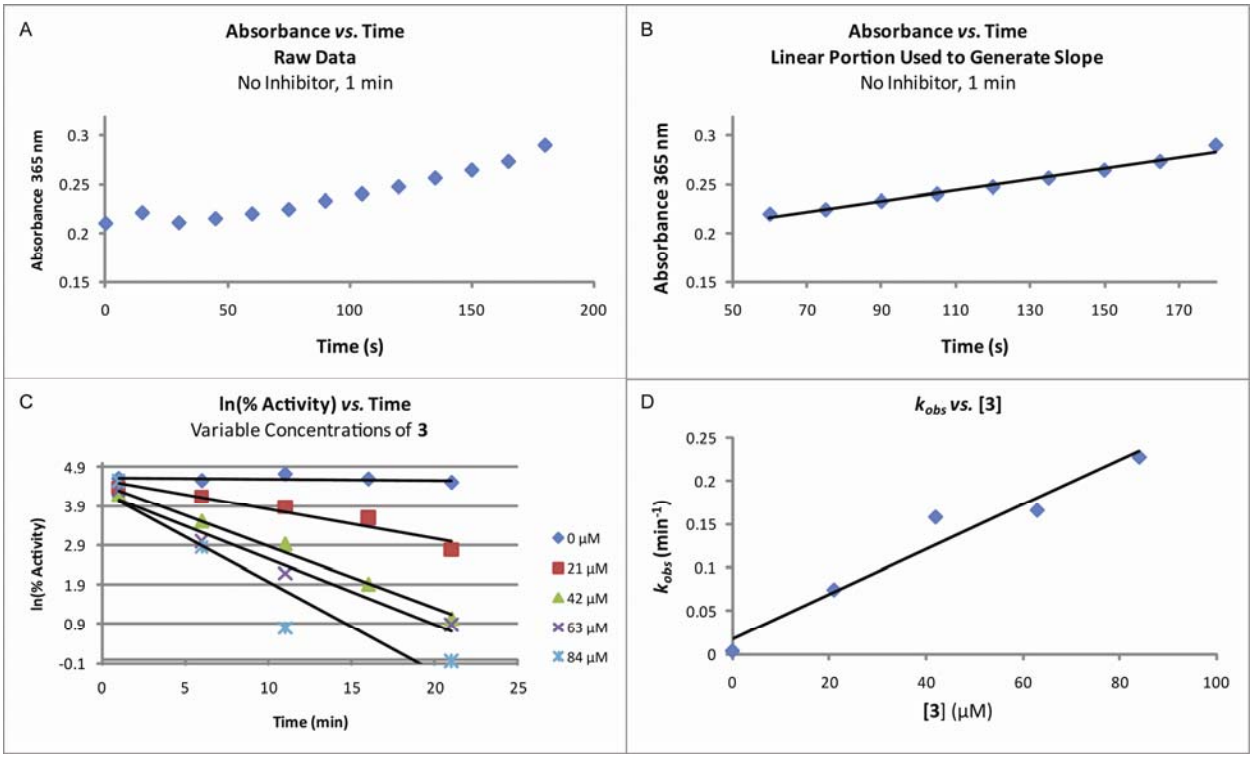

Figure S2. Representative ln(% Activity) *vs.* Time (min) plots for incubation of GlmS with potential time-dependent inhibitors. A) Representative plot showing time-dependent inhibition of GlmS on incubation with **3**. B) No time-dependent inhibition of GlmS is observed on incubation with 600 μM N_α-fumaramoyl-DAP (N_αFmmDAP). C) No time-dependent inhibition of GlmS is observed on incubation with 600 μM of the *N*-acyl-DAP dipeptides **1** or ***RR*-2**.

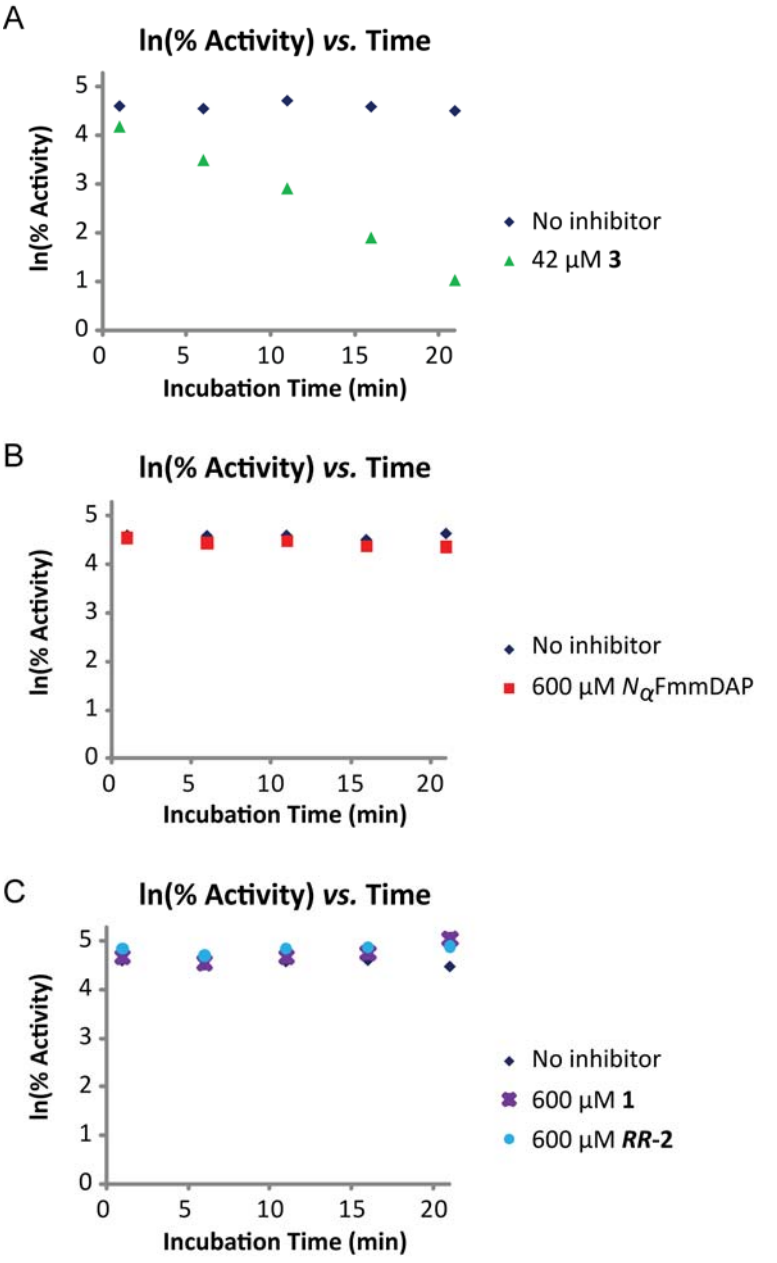

IV. MS Analysis of GlmS + Inhibitor Incubations

Method. *Reverse phase liquid chromatography-Fourier transform mass spectrometry analysis of GlmS covalent modification with inhibitors.*

Reaction mixtures (30 µL) contained 25 µM (50 µg) GlmS, 50 µM (for incubations containing **3** or ***RR*-4**) or 600 µM (for incubations containing ***SS*-4** or N_α-fumaramoyl-DAP) inhibitor, 1 mM TCEP, 10 mM Fru6P, 1 mM EDTA, and 100 mM potassium phosphate (pH 7.2). Reactions were incubated at room temperature for 2 hours, flash frozen in $N_2(l)$, and stored at -80 °C until trypsin digestion. The samples were thawed on ice, and then 30 µL 0.1 M NH_4HCO_3 was added to each sample. Trypsin (Promega Sequencing grade) was resuspended in the buffer provided by the manufacturer (50mM acetic acid) to a final concentration of 1 µg/µL and then added to the samples at a mass ratio of 1:5 trypsin:GlmS. The reactions were incubated at 30 °C for 15 min, and then quenched with one-half reaction volume of 25% formic acid and stored at -80 °C until MS analysis.

Chromatographic separation was achieved using a 75 µm x 100 mm C18 PicoFrit column (New Objective) on a Eksigent nano-capillary high pressure liquid chromatography (HPLC) system, with the gradient described in Table S1, where solvent A was water with 0.1% formic acid and solvent B was acetonitrile with 0.1% formic acid. The LC column was connected in-line with a Thermo Fisher Scientific LTQ-FT FTMS system operating at 7T. The instrument was calibrated each week and instrument parameters were tuned according to the manufacturer's instructions.

The MS method consisted of the following events: 1) FT scan, *m/z* 400–2,000, resolution 100,000, 2) data-dependent MS/MS on the top 3 peaks in each spectrum from scan event 1 using collision-induced dissociation (CID) with the following parameters: detection of all ions in the ion trap MS in centroid mode, isolation width 5 *m/z*, activation q value 0.25, activation time 30 ms, NCE 35. MS^3 analysis of the b_3 ion used CID with the following parameters: detection of all ions in the ion trap MS in centroid mode, isolation width 5 *m/z*, activation q value 0.25, activation time 30 ms, NCE 35. All data were analyzed using QualBrowser, part of the Xcalibur software packaged with the Thermo Fisher Scientific LTQ-FT.

Table S1. LC gradient for the separation of GlmS tryptic peptides.

Time (min)	%B
0	5
5	5
55	40
60	90
65	90
68	5
90	5

Figure S3. MS analysis of GlmS N-terminal tryptic decapeptide following incubation with no inhibitor.

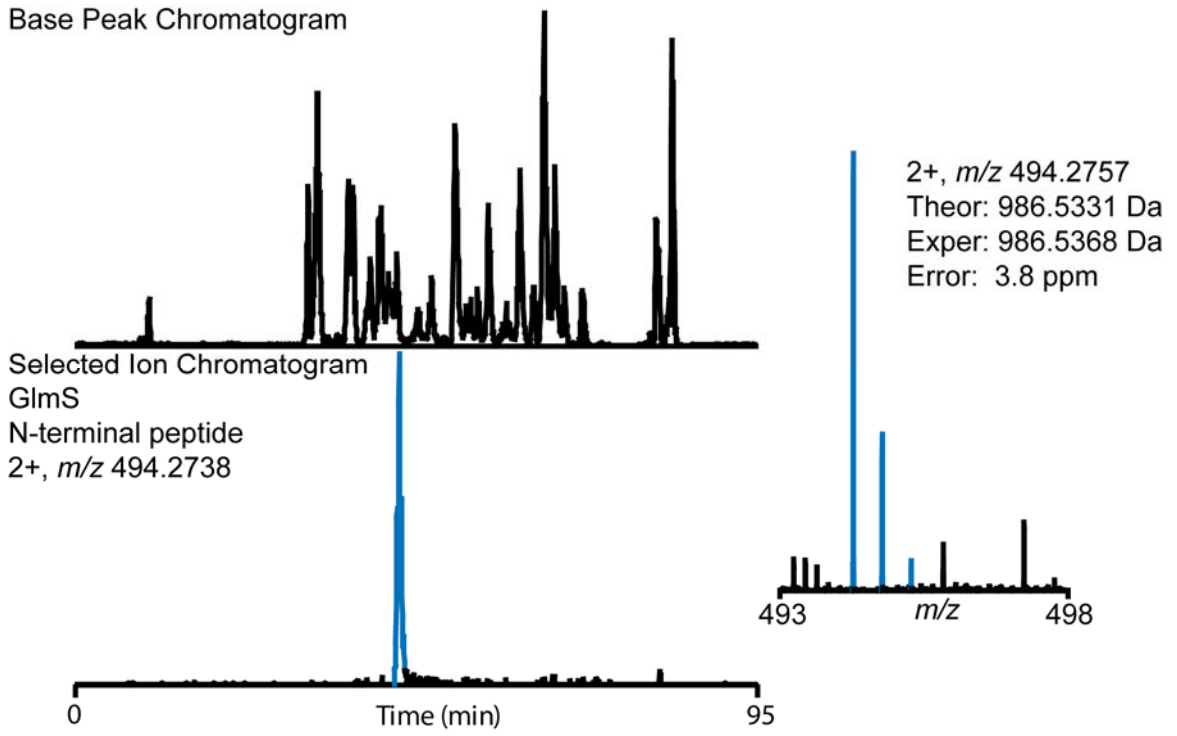

Figure S4. MS analysis of GlmS N-terminal tryptic decapeptides following incubation with compound **3**. The GlmS N-terminal tryptic peptide undergoes a mass shift of 201.1 Da on incubation with **3**.

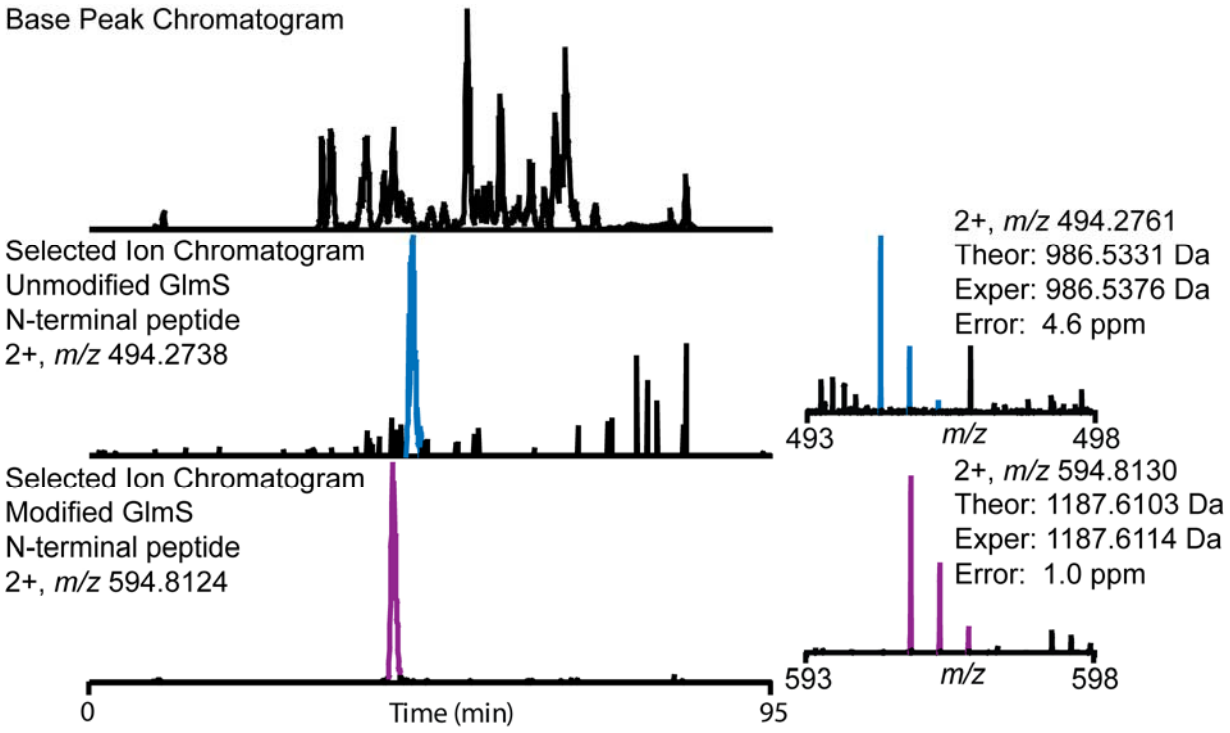

Figure S5. MS analysis of GlmS N-terminal tryptic decapeptides following incubation with compound ***RR*-4**. The GlmS N-terminal tryptic peptide undergoes a mass shift of 217.1 Da on incubation with ***RR*-4**.

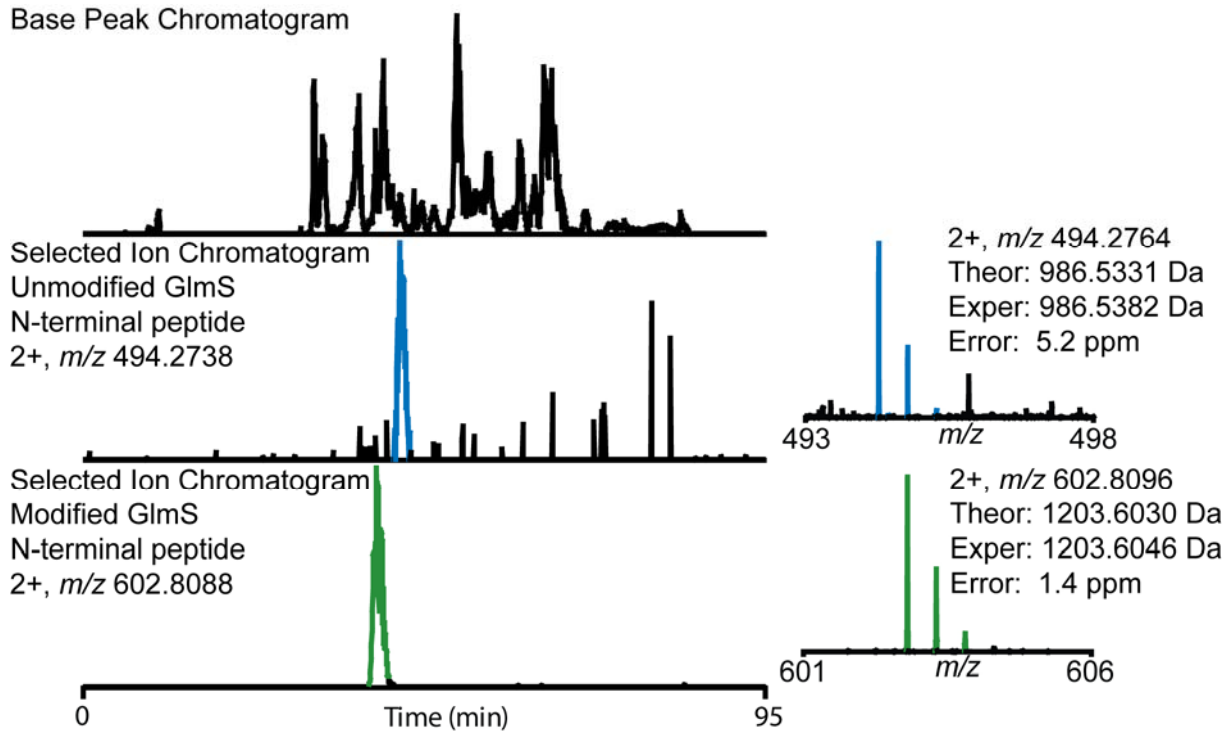

Figure S6. MS analysis of GlmS N-terminal tryptic decapeptides following incubation with compound ***SS*-4**. The GlmS N-terminal tryptic peptide undergoes a mass shift of 217.1 Da on incubation with ***SS*-4**.

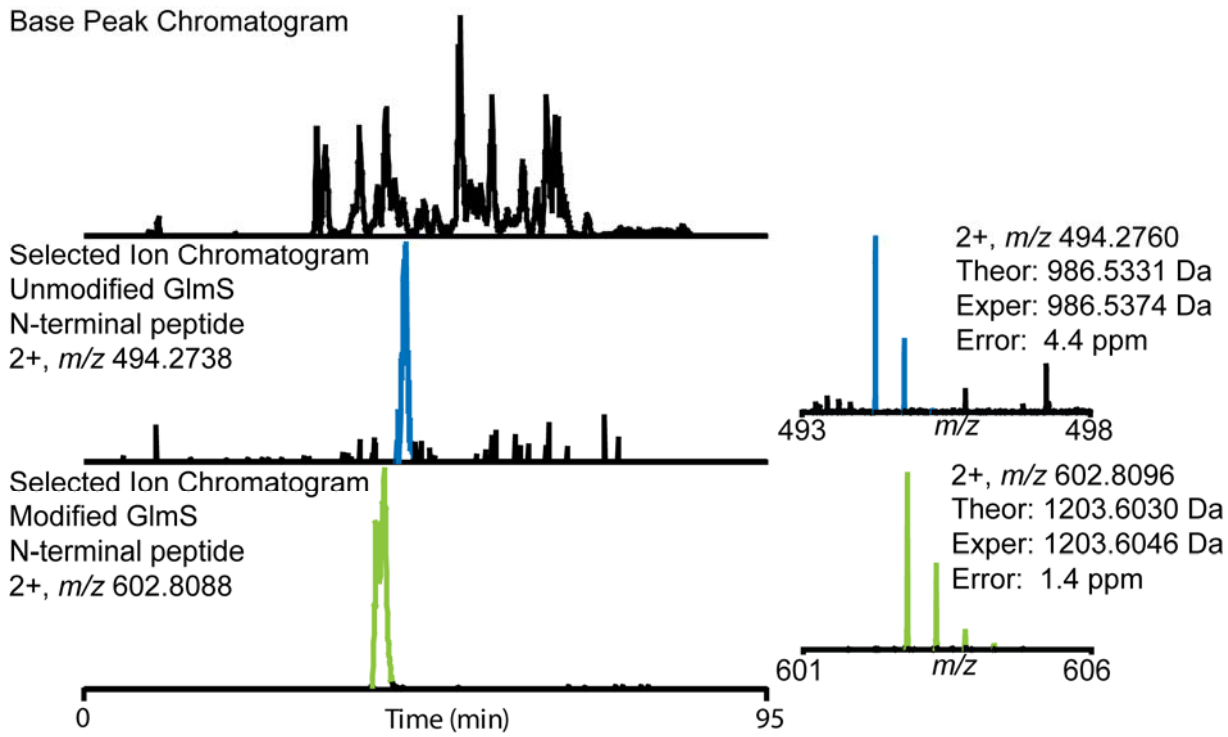

Figure S7. MS analysis of GlmS N-terminal tryptic decapeptides following incubation with N_α-fumaramoyl-DAP. The GlmS N-terminal tryptic peptide undergoes a mass shift of 201.1 Da on incubation with N_α-fumaramoyl-DAP. This compound may react slowly with GlmS such that modification was observed over the two hour incubation for the MS experiment but not over the 21 min time course of the *in vitro* inactivation assay (Figure S2B).

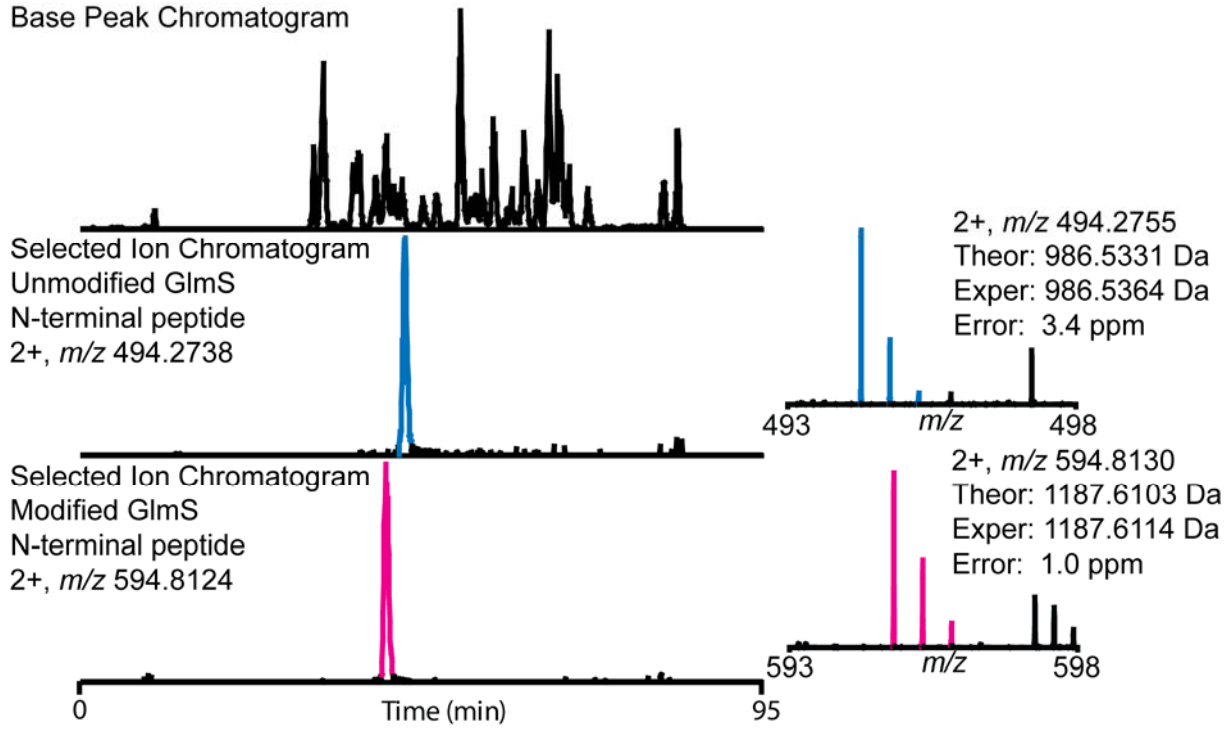

Table S2. Summary of GlmS N-terminal tryptic decapeptide masses observed in this study.

Decapeptide	Mass (Da, Theor)	Mass (Da, Exp)	Error (ppm)	Shift from unmodified GlmS (Da, Theor)	Shift from unmodified GlmS (Da, Exp)
Unmodified GlmS	986.5331	986.5368	3.8	0.00	0.00
GlmS + **3**	1187.6103	1187.6114	1.0	201.08	201.07
GlmS + ***RR*-4**	1203.6030	1203.6046	1.4	217.07	217.07
GlmS + ***SS*-4**	1203.6030	1203.6046	1.4	217.07	217.07
GlmS + N_α-fumaramoyl-DAP	1187.6103	1187.6114	1.0	201.08	201.07

Figure S8. MS/MS analysis of GlmS N-terminal tryptic decapeptides reveals mass shift of the b-ion series but not the y-ion series following incubation with compound **3**.

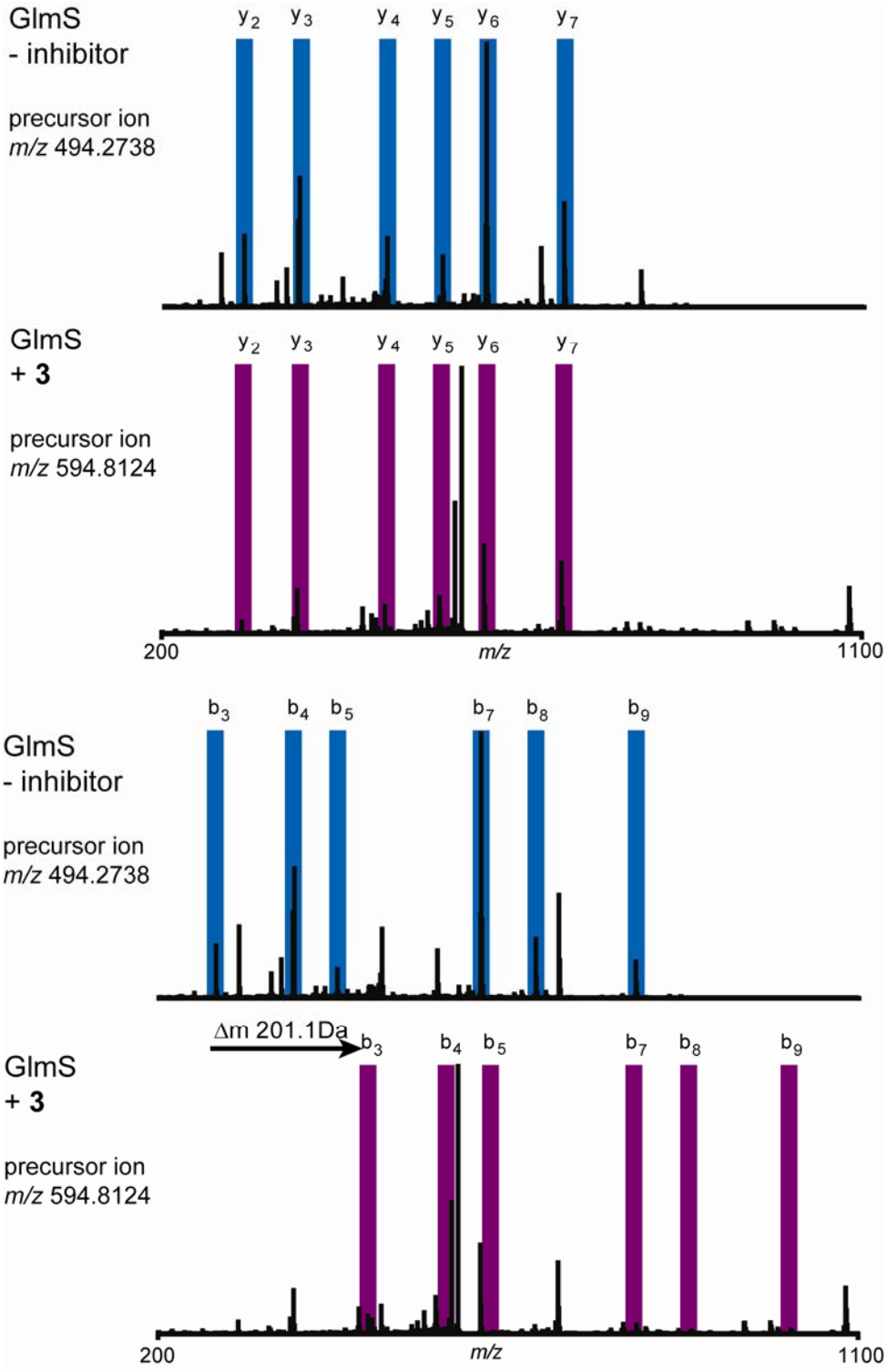

Figure S9. MS/MS analysis of GlmS N-terminal tryptic decapeptides reveals mass shift of the b-ion series but not the y-ion series following incubation with compound ***RR*-4**.

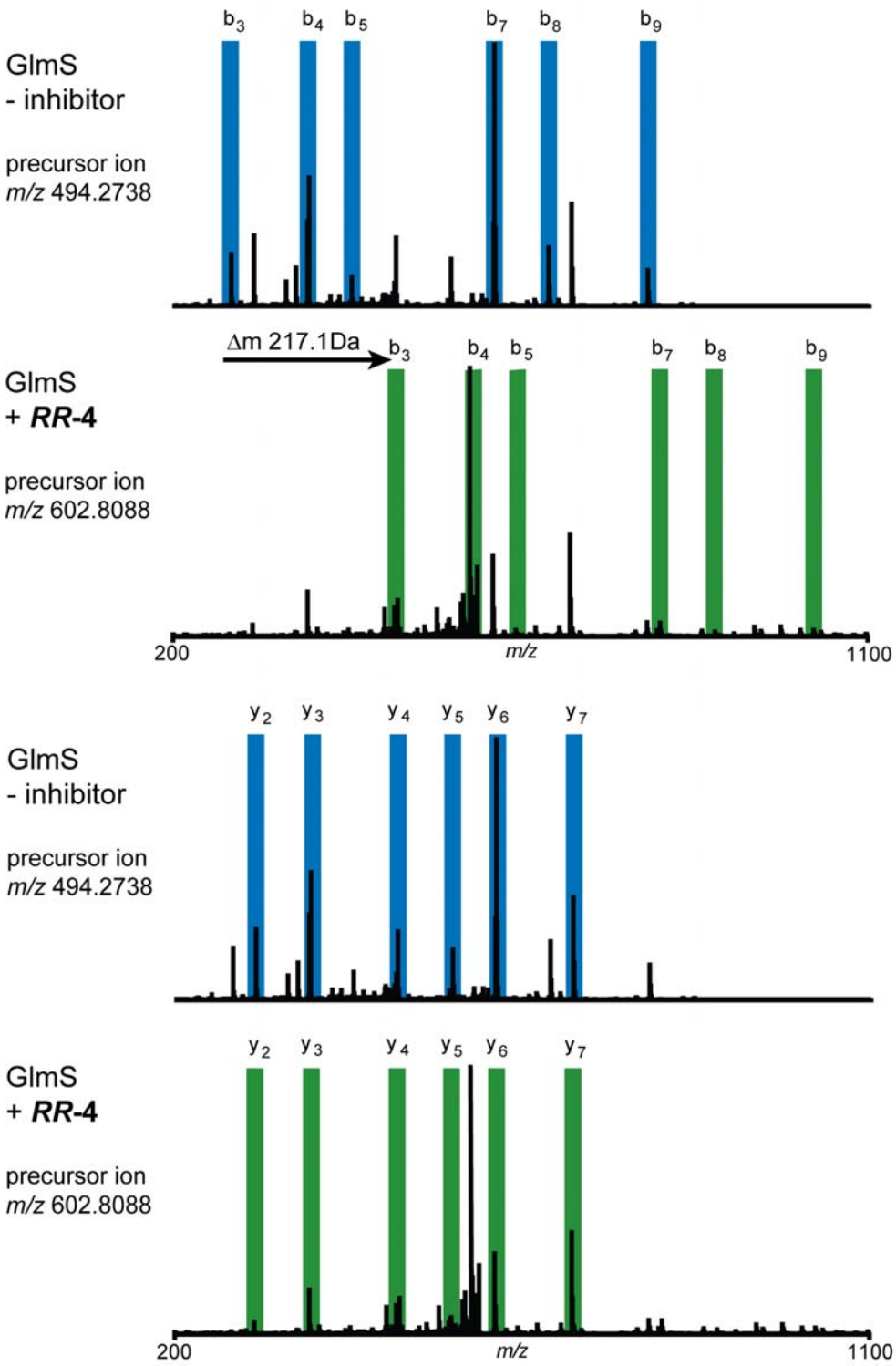

Figure S10. MS/MS analysis of GlmS N-terminal tryptic decapeptides reveals mass shift of the b-ion series but not the y-ion series following incubation with compound ***SS*-4**.

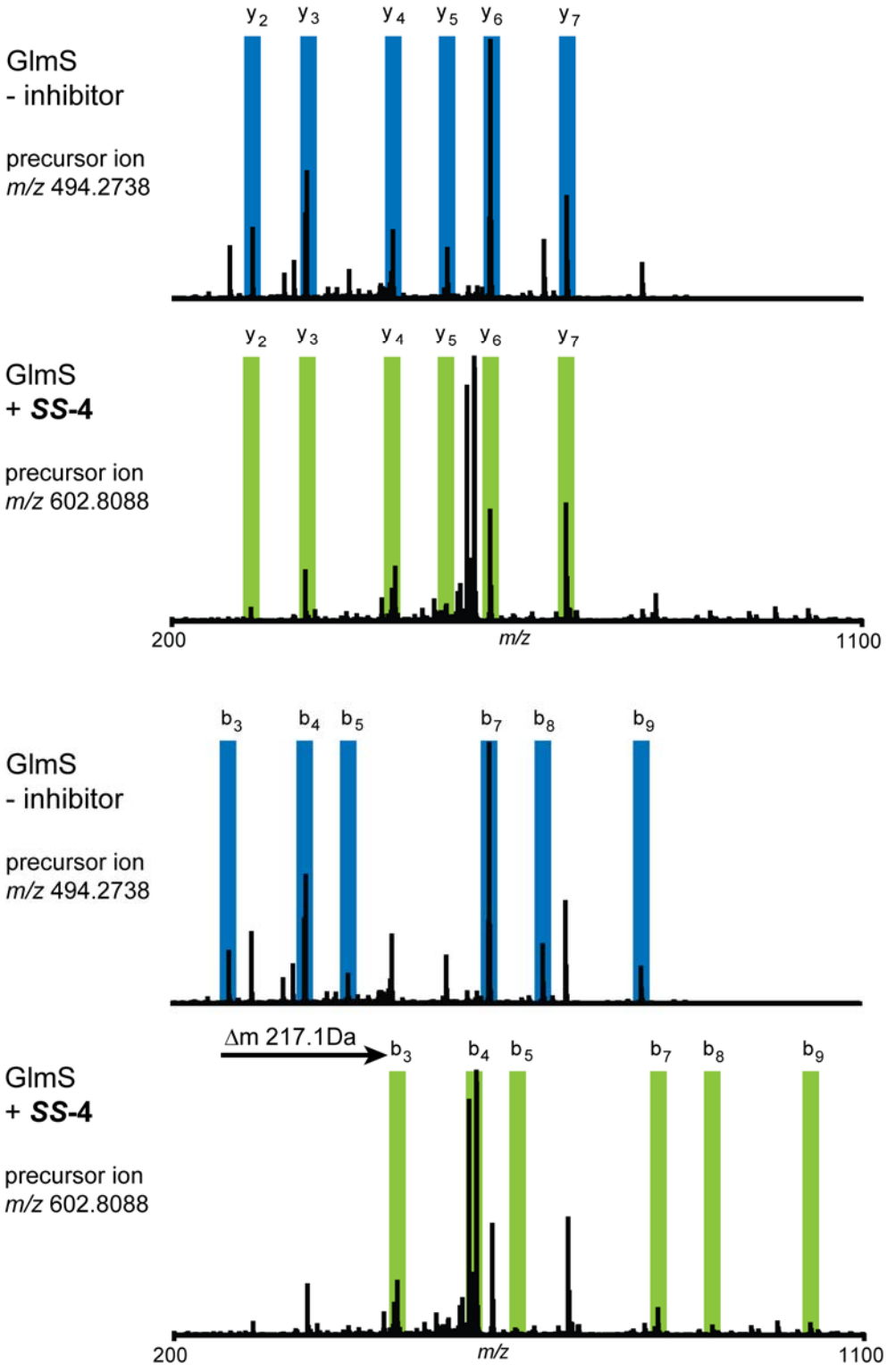

Figure S11. MS/MS analysis of GlmS N-terminal tryptic decapeptides reveals mass shift of the b-ion series but not the y-ion series following incubation with N_α-fumaramoyl-DAP (N_αFmmDAP).

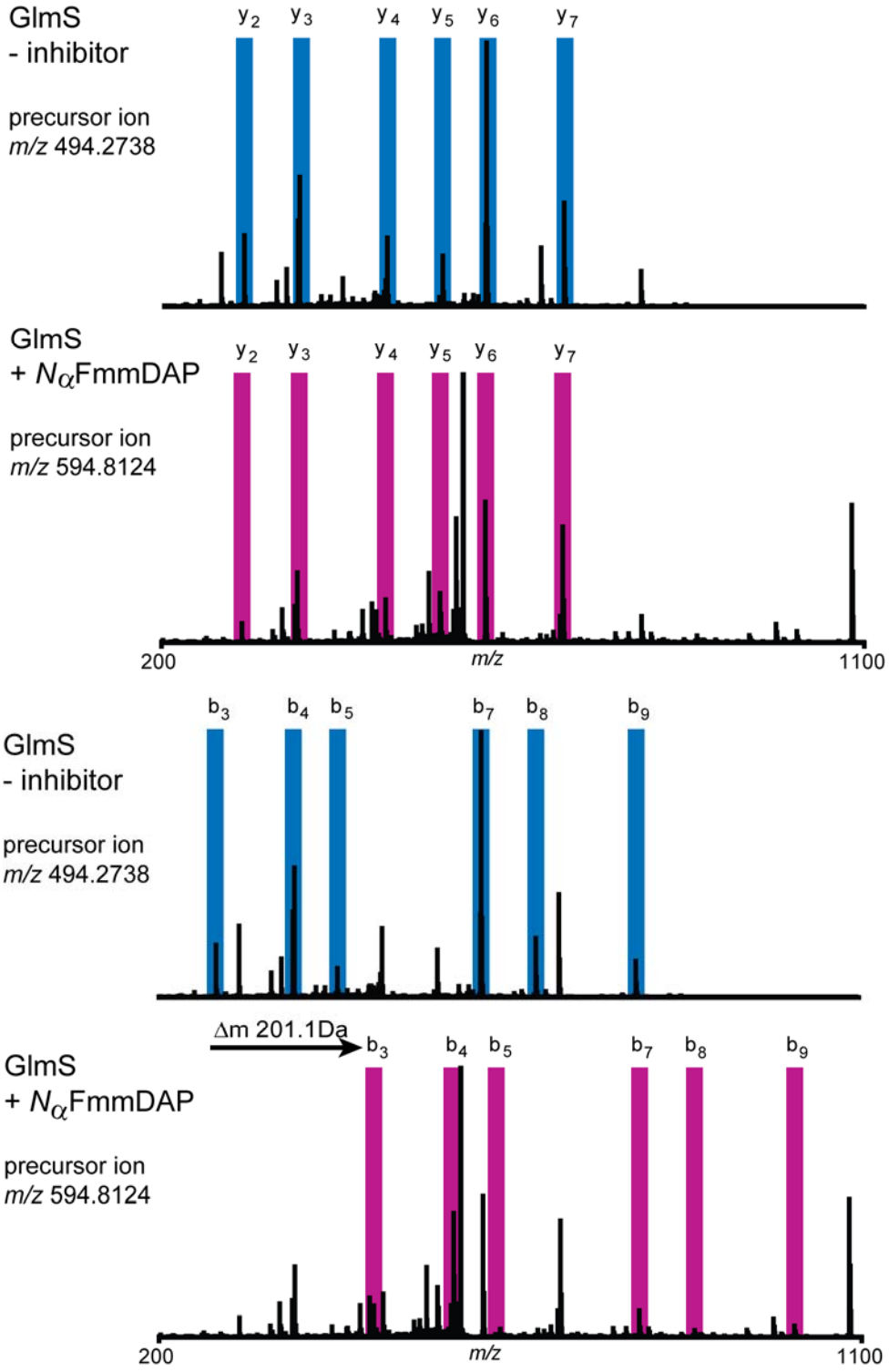

Figure S12. MS^3 analysis of GlmS N-terminal tryptic peptides localizes the site of modification with **3** to Cys1. MS^3 fragmentation of the modified CGI b_3 ion resulted in the formation of an ion with a mass consistent with the N-terminal CG b_2 ion in thioether linkage to **3** (teal), as well as two ions resulting from fragmentation of the thioether linkage (unmodified b_3 ion CGI is in pink and unmodified b_3 ion CGI after loss of H_2S is in orange). The observed *m/z* values for the highlighted peaks are 362.16 (teal), 274.14 (pink), and 240.14 (orange).

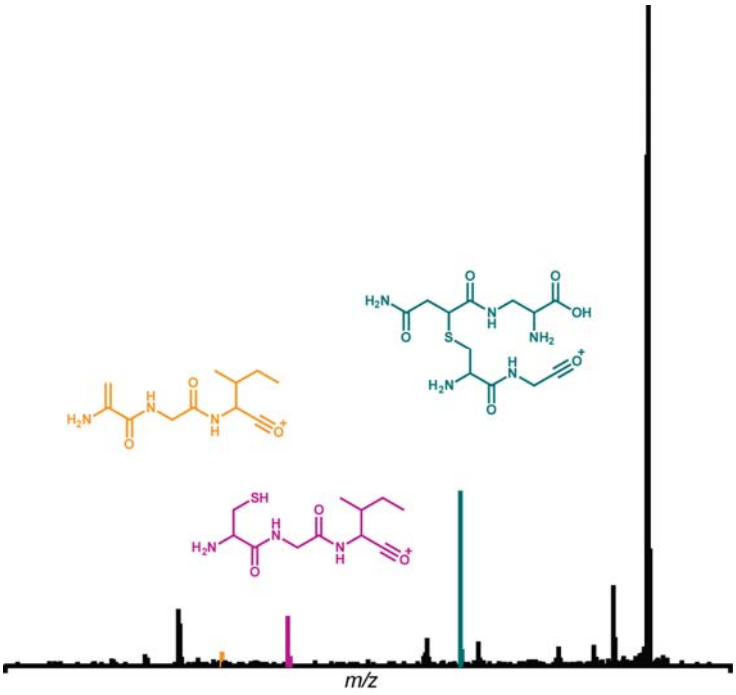

.

Figure S13. MS^3 analysis of GlmS N-terminal tryptic peptides localizes the site of modification with ***RR*-4** to Cys1. MS^3 fragmentation of the modified CGI b_3 ion resulted in the formation of an ion with a mass consistent with the N-terminal CG b_2 ion in thioether linkage to ***RR*-4** (teal), as well as two ions resulting from fragmentation of the thioether linkage (unmodified b_3 ion CGI is in pink and unmodified b_3 ion CGI after loss of H_2S is in orange). The observed *m/z* values for the highlighted peaks are 378.15 (teal) 274.11 (pink), and 240.09 (orange).

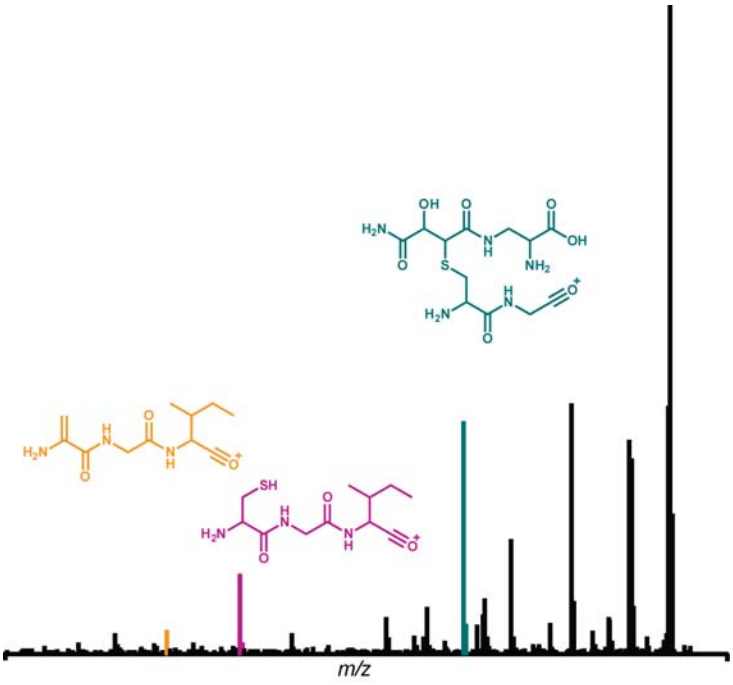

Figure S14. MS^3 analysis of GlmS N-terminal tryptic peptides localizes the site of modification with ***SS*-4** to Cys1. MS^3 fragmentation of the modified CGI b_3 ion resulted in the formation of an ion with a mass consistent with the N-terminal CG b_2 ion in thioether linkage to ***SS*-4** (teal), as well as two ions resulting from fragmentation of the thioether linkage (unmodified b_3 ion CGI is in pink and unmodified b_3 ion CGI after loss of H_2S is in orange). The observed *m/z* values for the highlighted peaks are 378.10 (teal) 274.12 (pink), and 240.11 (orange).

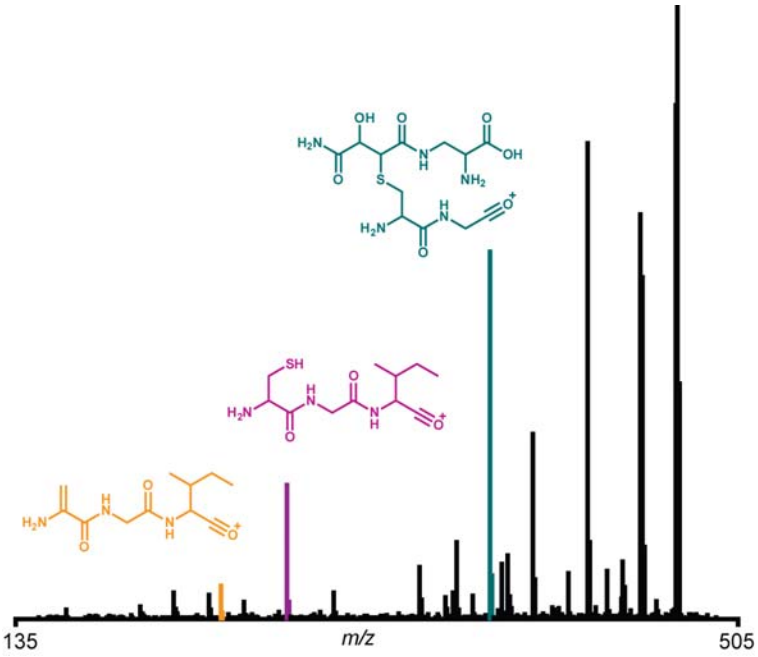

Figure S15. MS^3 analysis of GlmS N-terminal tryptic peptides localizes the site of modification with N_α-fumaramoyl-DAP to Cys1. MS^3 fragmentation of the modified CGI b_3 ion resulted in the formation of an ion with a mass consistent with the N-terminal CG b_2 ion in thioether linkage to N_α-fumaramoyl-DAP (teal), as well as two ions resulting from fragmentation of the thioether linkage (unmodified b_3 ion CGI is in pink and unmodified b_3 ion CGI after loss of H_2S is in orange). The observed *m/z* values for the highlighted peaks are 362.11 (teal) 274.14 (pink), and 240.17 (orange).

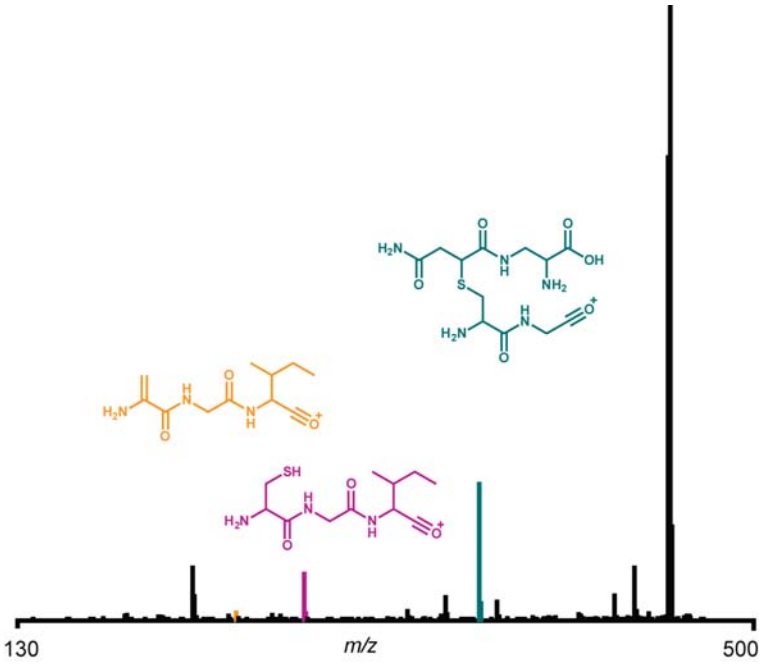

V. Minimum Inhibitory Concentration (MIC) Assays

Scheme S5. Preparation of ***RR*-2**.

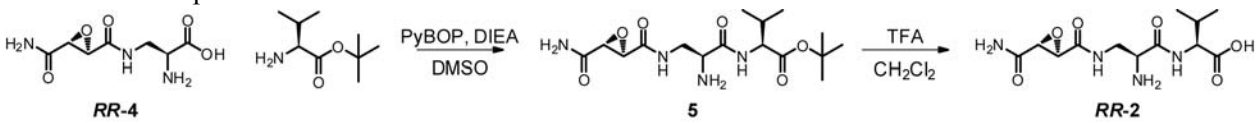

Method. *Preparation of* ***RR*-2**.

Chemicals used for synthesis were purchased from Sigma-Aldrich unless otherwise noted. Reported yields are unoptimized. Nuclear magnetic resonance (NMR) solvents were purchased from Cambridge Isotopes Laboratories. NMR spectra were recorded on a Varian 400 MHz or 600 MHz spectrometer. Chemical shifts are reported in parts-per-million (ppm) downfield from tetramethylsilane. For ^{1}H-NMR experiments, residual solvent resulting from incomplete deuteration served as the internal standard (methanol-d_4 δ 3.31).(*12*) For ^{13}C-NMR experiments, the solvent served as the internal standard (methanol-d_4 δ 49.15). NMR data are reported as follows: chemical shift, multiplicity (s = singlet, d = doublet, dd = doublet of doublets, m = multiplet), coupling constants, and integration. Mass spectrometry (MS) analysis was performed on an Agilent Technologies 6520 Accurate-Mass Q-TOF liquid chromatography (LC)-mass spectrometry (MS) instrument.

N_β-(*R,R*)-epoxysuccinamoyl-DAP-Val-O*t*bu (**5**). MH7-99

In a 50 mL pear flask with magnetic stir bar, N_β-(*R,R*)-epoxysuccinamoyl-DAP (***RR*-4)** (41.8 mg, 126 μmol, 1 equiv.) was dissolved in DMSO (15 mL). L-Val-O*t*bu (Fluka) (133 mg, 631 μmol, 5 equiv.) was added, followed by *N,N*-diisopropylethylamine (DIEA) (66 μL, 379 μmol, 3 equiv.), and then (benzotriazol-1-yloxy)tripyrrolidinophosphonium hexafluorophosphate (PyBOP) (75.2 mg, 145 μmol, 1.15 equiv.). The reaction was stirred at room temperature for 4 h. The reaction was diluted with ethyl acetate (EtOAc) (30 mL), and the solution was cooled to 0 °C in an ice bath. 2 mM ice cold HCl (30 mL) was added while the solution was on ice, and the organic layer was removed. The aqueous layer was washed with EtOAc (2 × 30 mL). The aqueous layer was placed on ice and 1 M ice cold NaOH added dropwise until the pH reached approximately 9.5. The aqueous layer was washed with EtOAc (2 × 30 mL) and then lyophilized overnight. The residue was dissolved in 3.5 mL H_2O and purified using a 10 mm × 100 mm Hypercarb column (Thermo Scientific) on a Beckman Coulter System Gold (126P solvent module, 168 detector) preparative HPLC and the absorbance was monitored at 220 nm. The compound eluted at approximately 38-40 min with the gradient described in Table S3, where solvent A was 100 mM triethylammonium acetate buffer in water (pH 7.0) and solvent B was CH_3CN. The compound was purified in 200-250 μL aliquots (attempts to purify larger volumes of crude material resulted in lack of separation between the desired compound peak and an impurity which eluted slightly later). A total of 1450 μL from the 3.5 mL crude solution was purified, HPLC fractions were lyophilized overnight, and then CH_3CN was added and removed *in vacuo* five times to remove most of the residual triethylamine to yield a white solid (8.1 mg, 20 μmol). Calculated μmol based on ^{1}H NMR estimation that the material consisted of a mixture of 1:0.35:0.1 (molar ratio) neutral product:protonated product acetate salt:triethylamine. ^{1}H NMR (600 MHz, METHANOL-d_4) δ ppm 0.99 (d, *J*=7.0 Hz, 3 H) 0.98 (d, *J*=7.0 Hz, 3 H) 1.49 (s, 9 H) 2.11 - 2.27 (m, 1 H) 3.42 (dd, *J*=13.8, 6.7 Hz, 1 H) 3.52 - 3.62 (m, 3 H) 3.62 - 3.69 (m, 1 H) 4.24 (d, *J*=5.3 Hz, 1 H). HRMS (ESI$^+$): $[M+H]^+$ *m/z* calcd. for $C_{16}H_{28}N_4O_6Na^+$, 395.1901 ; found, 395.1901.

Table S3. LC gradient for purification of **5**.

Time (min)	%B
0	0
10	0
45	40
48	90
53	90

N_{β}-(*R,R*)-epoxysuccinamoyl-DAP-Val (***RR*-2**).

In a 25 mL pear flask with magnetic stir bar, ester **5** (7.2 mg, 17 μmol, 1 equiv.) was dissolved in dichloromethane (12 mL). The solution was stirred at 0 °C. Trifluoroacetic acid (TFA) (3 mL) was added dropwise to the stirring solution. The solution was warmed to room temperature and stirred at room temperature overnight. Solvent and TFA were removed *in vacuo* to afford a white solid (7.5 mg, 100% yield). ^{1}H NMR (600 MHz, METHANOL-d_4) δ ppm 1.01 (d, *J*=7.0 Hz, 3 H) 1.03 (d, *J*=7.0 Hz, 3 H) 2.22 - 2.32 (m, 1 H) 3.56 (d, *J*=1.8 Hz, 1 H) 3.57 (d, *J*=1.8 Hz, 1 H) 3.67 (dd, *J*=14.7, 5.9 Hz, 1 H) 3.81 (dd, *J*=14.7, 4.7 Hz, 1 H) 4.12 (dd, *J*=5.9, 4.7 Hz, 1 H) 4.40 (d, *J*=5.3 Hz, 1 H). ^{13}C NMR (151 MHz, METHANOL-d_4) δ ppm 18.30, 19.67, 31.45, 41.17, 54.48, 54.91, 54.97, 59.68, 168.51, 170.57, 171.31, 174.68. HRMS (ESI$^+$): $[M+H]^+$ *m/z* calcd. for $C_{12}H_{21}N_4O_6^+$; 317.1456 found, 317.1449.

Method. *MIC determination.*

5 mL cultures were grown for approximately 24 hours at 30 °C for *E. amylovora* 273 and at 37 °C for *E. coli* K12 MG1655 and *E. coli* NR698. The cultures were diluted 1:1,000 into *E. coli* minimal medium (prepared by dissolving 0.25 g yeast extract, 20 mL glycerol, 4 g K_2HPO_4, 1.72 g KH_2PO_4, 0.5 g NaCl, 2 g $(NH_4)_2SO_4$, 0.2 g sodium citrate, 0.02 g $MgSO_4 \cdot 7H_2O$ in 1 L of water and then filtering through a 0.2 μm filter). 150 μL of the diluted culture was transferred to the wells of a 96-well plate. Serial 1:1 dilutions of **1** or ***RR*-2** in DMSO (1.5 uL) or ***RR*-4** in water (30 uL) were added to each well of the culture plate. In each row treated with **1** or ***RR*-2**, one well was treated with 1.5 uL 100% DMSO and one with 1.5 uL 50 mg/mL carbenicillin. In each row treated with ***RR*-4**, one well was treated with 30 uL 100% water and one with 30 uL 50 mg/mL carbenicillin. For *N*-acetylglucosamine (GlcNAc) experiments, GlcNAc was added to each well to a final concentration of 167 mM.

The plates were incubated with shaking at 30 °C (*E. amylovora*) or 37 °C (*E. coli* K12 and NR698) for 13 hours. The $OD_{600\ nm}$ was read on a Molecular Devices SpectraMax 340PC384 plate reader. OD values were converted to % values relative to the 100% DMSO well in the same row. MICs were defined as the lowest test compound concentration that resulted in an increase of less than 10 of the converted % value over the adjacent carbenicillin well. Reported MICs are the median values of replicate experiments. *E. amylovora* experiments were carried out in compliance with USDA regulations.

Table S4. MIC values for **1**, ***RR*-2**, and ***RR*-4** against *E. amylovora* 273, *E. coli* K12 MG1655, and *E. coli* NR698.[1] GlcNAc = *N*-acetylglucosamine, ND = not determined.

MIC Values			**Organism**		
Antibiotic		167 mM GlcNAc	*E. amylovora* 273	*E. coli* K12 MG1655	*E. coli* NR698
1	Dapdiamide A	-	188 μM (78 μg/mL)	> 500 μM (> 207 μg/mL)	188 μM (78 μg/mL)
		+	> 417 μM (> 173 μg/mL)	ND	> 417 μM (> 173 μg/mL)
***RR*-2**	N_{β}-*R,R*-Epoxysuccinamoyl-DAP-Val	-	12 μM (5 μg/mL)	> 500 μM (> 215 μg/mL)	16 μM (7 μg/mL)
		+	> 417 μM (> 179 μg/mL)	ND	> 417 μM (> 179 μg/mL)
***RR*-4**	N_{β}-*R,R*-Epoxysuccinamoyl-DAP	-	> 417 μM (> 138 μg/mL)	ND	> 417 μM (> 138 μg/mL)

[1] MIC values were not determined for **3** as the compound was only soluble in concentrations of borate·NaOH, pH 9.5 that inhibited *E. coli* growth.

VI. References

1. Dawlaty, J., Zhang, X., Fischbach, M. A., and Clardy, J. (2010) *J. Nat. Prod. 73*, 441-446.
2. Shoji, J., Hinoo, H., Sakazaki, R., Kato, T., Hattori, T., Matsumoto, K., Tawara, K., Kikuchi, J., and Terui, Y. (1989) *J. Antibiot. 42*, 869-874.
3. Sammer, U. F., Volksch, B., Mollmann, U., Schmidtke, M., Spiteller, P., Spiteller, M., and Spiteller, D. (2009) *Appl. Environ. Microbiol. 75*, 7710-7717.
4. Molloy, B. B., Lively, D. H., Gale, R. M., Forman, M., Boeck, L. D., Higgens, C. E., Kastner, R. E., Huckstep, L. L., and Neuss, N. (1972) *J. Antibiot. 25*, 137-140.
5. van der Baan, J. L., Barnick, J. W. F. K., and Bickelhaupt, F. (1983) *J. Antibiot. 36*, 784-792.
6. Cooper, R., Horan, A. C., Gentile, F., Gullo, V., Loebenberg, D., Marquez, J., Patel, M., Puar, M. S., and Truumees, I. (1988) *J. Antibiot. 41*, 13-19.
7. Rane, D. F., Girijavallabhan, V. M., Ganguly, A. K., Pike, R. E., Saksena, A. K., and McPhail, A. T. (1993) *Tetrahedron Lett. 34*, 3201-3204.
8. Hollenhorst, M. A., Clardy, J., and Walsh, C. T. (2009) *Biochemistry 48*, 10467-10472.
9. Hollenhorst, M. A., Bumpus, S. B., Matthews, M. L., Bollinger, J. M., Kelleher, N. L., and Walsh, C. T. (2010) *J. Am. Chem. Soc. 132*, 15773-15781.
10. Valerio-Lepiniec, M., Aumont-Nicaise, M., Roux, C., Raynal, B., England, P., Badet, B., Badet-Denisot, M.-A., and Desmadril, M. (2010) *Arch. Biochem. Biophys. 498*, 95-104.
11. Badet, B., Vermoote, P., and Le Goffic, F. (1988) *Biochemistry 27*, 2282-2287.
12. Gottlieb, H. E., Kotlyar, V., and Nudelman, A. (1997) *J. Org. Chem 62*, 7512-7515.